Proceedings of IMECE'03
2003 ASME International Mechanical Engineering Congress and Exposition
November 16-21, 2003, Washington, D.C. USA

IMECE2003-41825

OPTIMAL ROLLOVER PREVENTION WITH STEER BY WIRE AND DIFFERENTIAL BRAKING

Christopher R. Carlson
Stanford University
Mechanical Engineering
Stanford, CA 94305-4021, USA
crcarlson@stanford.edu

J. Christian Gerdes
Stanford University
Mechanical Engineering
Stanford, CA 94305-4021, USA
gerdes@cdr.stanford.edu

ABSTRACT

This paper uses Model Predictive Control theory to develop a framework for automobile stability control. The framework is then demonstrated with a roll mode controller which seeks to actively limit the peak roll angle of the vehicle while simultaneously tracking the driver's yaw rate command. Initially, control law presented assumes knowledge of the complete input trajectory and acts as a benchmark for the best performance any controller could have on this system. This assumption is then relaxed by only assuming that the current driver steering command is available. Numerical simulations on a nonlinear vehicle model show that both control structures effectively track the driver intended yaw rate during extreme maneuvers while also limiting the peak roll angle. During ordinary driving, the controlled vehicle behaves identically to an ordinary vehicle. These preliminary results show that for double lane change maneuvers, it is possible to limit roll angle while still closely tracking the driver's intent.

NOMENCLATURE

U_x Longitudinal velocity (Body fixed frame)
U_y Lateral velocity (Body fixed frame)
$\dot{\psi}$ Yaw rate
ϕ Roll Angle
$\dot{\phi}$ Roll Angle rate
α_f,α_r Front and rear tire Slip Angle
δ Steering Angle
m Mass
I_{xx} Moment of inertia about the x axis
a Distance from front axle to c.g.
b Distance from rear axle to c.g.
d Track width
h_{CG} Lumped height of roll mode
h Discrete control horizon length
F_x, F_y Longitudinal and lateral force on a wheel
V Longitudinal velocity for model linearization
C_{yf}, C_{yr} Front and rear cornering stiffness
C_0, C_1, C_2 Lumped bicycle model parameters defined in the text
t Time
Δt Discrete sampling period
A State transition matrix
B Input direction matrix
C Controlled trajectory output matrix
$\bar{C}$ Reference trajectory output matrix
$\check{C}$ Constrained trajectory output matrix
k Current discrete sample step
$r(t)$ Reference input for control law

1 Introduction

The composition of the current automotive fleet consists of 36% light trucks, minivans and sport utility vehicles (SUVs). Unfortunately, the rate of fatal rollovers for pickups is twice that for passenger cars and the rate for SUVs is almost three times the passenger car rate. While rollover only affects about three percent of passenger vehicles involved in crashes, it accounts for 32 percent of passenger vehicle occupant fatalities [1]. These statistics motivate a very real opportunity to improve passenger

vehicle safety by preventing vehicle rollover via active stability control.

The vehicle control community observes that ordinary drivers rarely push their vehicle to the limits and are often unprepared for vehicle response during extreme maneuvers. This motivates the need for driver assistance technology which is transparent to the driver during normal driving, which also ensures the vehicle response is intuitive during extreme maneuvers. Current production vehicles commonly use differential braking technology to limit vehicle sideslip angle during extreme maneuvers [2]. Differential braking may also be used to prevent vehicle rollover [3, 4] and production rollover prevention systems of this sort are already on the market.

These control laws have proven to effectively limit the peak roll angle of a vehicle while working with limited feedback information such as; steering angle, yaw rate, lateral acceleration and brake pressure. However, these control laws do not prioritize driver control intent and may create nonintuitive vehicle behavior at the limits. This paper takes advantage of recent developments in GPS sensing technology which allows accurate measurement of additional vehicle states, including; sideslip, yaw rate, roll angle and roll rate [5–7]. These measurements represent full state feedback for the control laws presented here and enable more advanced control techniques than are currently feasible.

Current automotive control systems also have limited actuator authority, usually centered around brake pressure control and sensing. These actuation schemes do not have a good measurement of the forces generated by the tires and rely on control schemes which are extremely robust to tire parameters [2]. This work, however, assumes a very good estimate of tire longitudinal tire properties using GPS and stock ABS sensors [8]. These estimates enable more precise control of tire forces than is currently available for modern automotive control systems. Furthermore, this paper assumes the controlled vehicle is steer-by-wire and that there is no physical connection between the steering wheel and the tires.

Full state feedback and detailed knowledge of the tire properties enables more advanced control techniques which were previously impractical for automotive applications. This paper presents a vehicle stability control framework based upon Model Predictive Control (MPC). This control framework has a great history of success in the process control industries [9] and enforces many useful actuator and state constraints. In particular, it explicitly accounts for output and actuator saturation, both of which are inherent to physical vehicles. Historically, this control strategy has been limited to systems with slow dynamics due to the computational load required at each time step. However, recent advances in MPC theory allow the computation of the control law to be explicitly performed off-line [10, 11]. This new theory enables MPC for automotive systems which have fast dynamics and practically limited computational power.

This paper presents two MPC control laws and studies their performance via numerical simulation. The first control law assumes complete knowledge of the driver's command input in advance. Although impractical, it sets a benchmark for the best performance achievable by any control law. This control law performs extremely well in simulation and suggests that it should be possible to safely limit the peak roll angle while also following the driver's command. The second, more practical, control law assumes a zero order hold on the driver command and implements a receding horizon control scheme which is recalculated at every time step. It also performs quite well in simulation with nonlinear tires and nonlinear vehicle dynamics.

The computational complexity of the MPC control schemes grows quite rapidly with horizon length and state dimension. However, for the simulations presented there, the control action suggests that a very simple control logic may take the place of the complex control structure. This is one of the subjects for future research for this system.

2 Vehicle Modeling

2.1 Nonlinear Dynamics

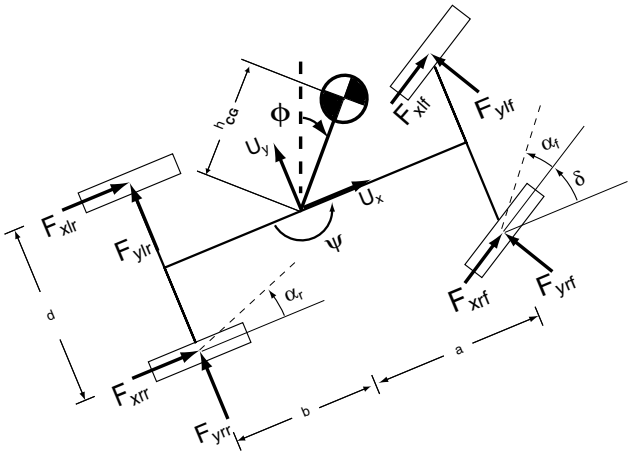

Figure 1. 4 wheel vehicle model with roll

Figure 1 shows a schematic diagram for a planar vehicle model with a roll mode. a and b are the distances from the vehicle axles to the center of gravity (CG), d is the rear track width and h_{CG} is the height of the CG. α_f and α_r are the vehicle sideslip angles at the front and rear axles respectively. m is the mass of the vehicle, which is assumed to have no unsprung mass, and I_{xx}, I_{yy}, I_{zz} are the moments of inertia about the roll, pitch and yaw axes respectively. The forces acting upon the vehicle lie either along the tire axis of heading or perpendicular to it. The vehicle states are chosen to be:

$$Ux \triangleq \text{Longitudinal velocity} \tag{1}$$

$$U_y \triangleq \text{Lateral velocity} \tag{2}$$

$$\dot{\psi} \triangleq \text{Yaw rate} \tag{3}$$

$$\dot{\phi} \triangleq \text{Roll rate} \tag{4}$$

$$\phi \triangleq \text{Roll angle} \tag{5}$$

With these definitions, the equations of motion may be written in the vehicle fixed frame,

$$\begin{aligned}
\dot{Ux} = & \frac{F_{xr}+F_{xf}\cos(\delta)-F_{yf}\sin(\delta)}{m}+U_y\dot{\psi} \\
& +\frac{\left\{F_{xr}+F_{xf}\cos(\delta)-F_{yf}\sin(\delta)\right\}h_{CG}^2\sin^2(\phi)}{I_{yy}\sin^2(\phi)+I_{zz}\cos^2(\phi)} \\
& -\frac{\left\{a\left(F_{yf}\cos(\delta)+F_{xf}\sin(\delta)\right)-bF_{yr}\right\}h_{CG}\sin\phi}{I_{yy}\sin^2(\phi)+I_{zz}\cos^2(\phi)} \\
& -\frac{\left\{(F_{xrr}-F_{xlr})\frac{d}{2}+(F_{xrf}-F_{xlf})\frac{d}{2}\cos(\delta)\right\}h_{CG}\sin\phi}{I_{yy}\sin^2(\phi)+I_{zz}\cos^2(\phi)} \\
& -\frac{2I_{zz}h_{CG}\cos(\phi)\dot{\psi}\dot{\phi}}{I_{yy}\sin^2(\phi)+I_{zz}\cos^2(\phi)}
\end{aligned} \tag{6}$$

$$\begin{aligned}
\dot{U_y} = & \frac{\left\{I_{xx}+h_{CG}^2m\right\}}{I_{xx}+mh_{CG}^2\sin^2(\phi)}\left(\frac{F_{yr}+F_{yf}\cos(\delta)+F_{xf}\sin(\delta)}{m}\right) \\
& -\frac{\left\{I_{xx}+h_{CG}^2m\right\}}{I_{xx}+mh_{CG}^2\sin^2(\phi)}\left(h_{CG}\sin(\phi)\dot{\phi}^2\right) \\
& +\frac{\left\{mgh_{CG}\sin(\phi)-k\phi-b\dot{\phi}\right\}h_{CG}\cos(\phi)}{I_{xx}+mh_{CG}^2\sin^2(\phi)} \\
& -Ux\dot{\psi}-h_{CG}\sin(\phi)\dot{\psi}^2 \\
& +\frac{\left\{(I_{yy}-I_{zz})\cos^2(\phi)\right\}h_{CG}\sin(\phi)\dot{\psi}^2}{I_{xx}+mh_{CG}^2\sin^2(\phi)}
\end{aligned} \tag{7}$$

$$\begin{aligned}
\ddot{\psi} = & \frac{a\left\{F_{yf}\cos(\delta)+F_{xf}\sin(\delta)\right\}-bF_{yr}}{I_{yy}\sin^2(\phi)+I_{zz}\cos^2(\phi)} \\
& +\frac{(F_{xrr}-F_{xlr})\frac{d}{2}+(F_{xrf}-F_{xlf})\frac{d}{2}\cos(\delta)}{I_{yy}\sin^2(\phi)+I_{zz}\cos^2(\phi)} \\
& -\frac{\left\{F_{xr}+F_{xf}\cos(\delta)-F_{yf}\sin(\delta)\right\}h_{CG}\sin(\phi)}{I_{yy}\sin^2(\phi)+I_{zz}\cos^2(\phi)} \\
& -\frac{2(I_{yy}-I_{zz})\sin(\phi)\cos(\phi)\dot{\psi}\dot{\phi}}{I_{yy}\sin^2(\phi)+I_{zz}\cos^2(\phi)}
\end{aligned} \tag{8}$$

$$\begin{aligned}
\ddot{\phi} = & \frac{mgh_{CG}\sin(\phi)-k\phi-b\dot{\phi}}{I_{xx}+mh_{CG}^2\sin^2(\phi)} \\
& +\frac{\left\{F_{yr}+F_{yf}\cos(\delta)+F_{xf}\sin(\delta)\right\}h_{CG}\cos(\phi)}{I_{xx}+mh_{CG}^2\sin^2(\phi)} \\
& +\frac{\left\{(I_{yy}-I_{zz})\dot{\psi}^2-mh_{CG}^2\dot{\phi}^2\right\}\sin(\phi)\cos(\phi)}{I_{xx}+mh_{CG}^2\sin^2(\phi)}
\end{aligned} \tag{9}$$

2.2 Nonlinear Tires

The nonlinear model used to verify the control laws uses the HSRI tire model [12],

$$\mu = \mu_{peak}\left((1-A_sR\omega\sqrt{s^2+\tan^2\alpha}\right) \tag{10}$$

$$H = \sqrt{\left[\frac{C_xs}{\mu F_z(1-s)}\right]^2+\left[\frac{C_y\tan\alpha}{\mu F_z(1-s)}\right]^2} \tag{11}$$

$$F_x = \begin{cases} C_x\frac{s}{1-s} & : \quad H<\frac{1}{2} \\ C_x\frac{s}{1-s}\left(\frac{1}{H}-\frac{1}{4H^2}\right) & : \quad H\geq\frac{1}{2} \end{cases} \tag{12}$$

$$F_y = \begin{cases} C_y\frac{1}{1-s}\tan(\alpha) & : \quad H<\frac{1}{2} \\ C_y\frac{1}{1-s}\left(\frac{1}{H}-\frac{1}{4H^2}\right)\tan(\alpha) & : \quad H\geq\frac{1}{2} \end{cases} \tag{13}$$

where C_x and C_y are the longitudinal and cornering stiffnesses, s denotes tire slip, μ_{peak} denotes peak road friction (assumed to be 0.9 for this work), A_s is a friction discount factor due to sliding in the patch ($A_s = 0.02$ for this work), R, ω are the tire effective radius and angular velocity, and F_x, F_y are calculated for each tire. Figure 2 shows representative tire curves from this model for a single axle.

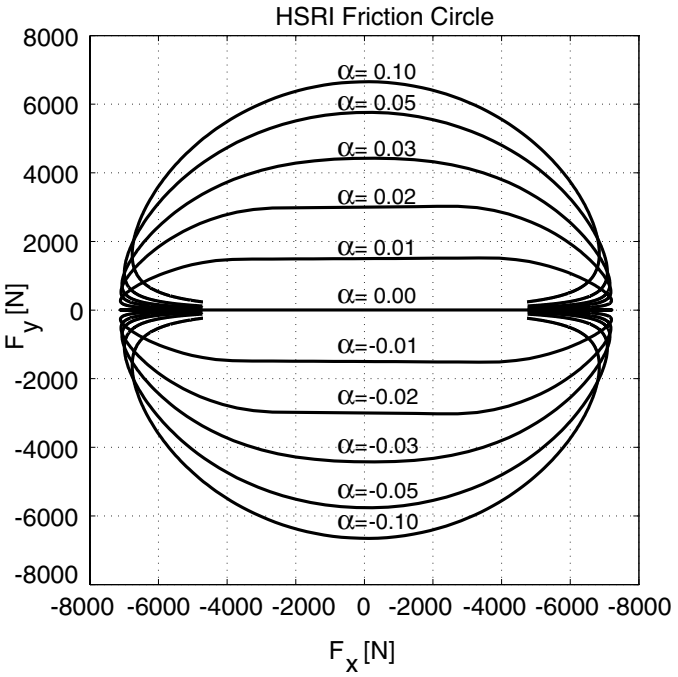

Figure 2. HSRI tire model friction circle

2.3 Linear vehicle Model

Although the nonlinear model is linearized for control, the full nonlinear model with nonlinear tires is used to verify the actions of the control law in simulation.

For linearization, this model assumes a constant longitudinal velocity U_x.

$$U_x = V \tag{14}$$
$$\dot{U}_x = 0 \tag{15}$$

A new variable β is introduced as a state which describes the sideslip angle at the center of gravity of the vehicle for small angles.

$$\beta = \tan^{-1}\frac{U_y}{V} \tag{16}$$
$$\cong \frac{U_y}{V} \tag{17}$$
$$\dot{\beta} \cong \frac{\dot{U}_y}{V} \tag{18}$$

The forces on the tires are modeled as proportional to the slip angles at each axle. C_{yf} and C_{yr} are the cornering stiffnesses of the front and rear tires respectively.

$$F_{yr} = -C_{yr}\left\{\beta - \frac{b}{V}\dot{\psi}\right\} \tag{19}$$
$$F_{yf} = -C_{yf}\left\{\beta + \frac{a}{V}\dot{\psi} - \delta\right\} \tag{20}$$

Finally, for convenience, the following constants are defined.

$$C_0 = C_{yf} + C_{yr} \tag{21}$$
$$C_1 = aC_{yf} - bC_{yr} \tag{22}$$
$$C_2 = a^2C_{yf} + b^2C_{yr} \tag{23}$$
$$I_{eq} = I_{xx} + h^2m \tag{24}$$

By linearizing about small angles, the following four state linear model may be defined,

$$\begin{bmatrix}\dot{\beta}\\ \ddot{\psi}\\ \dot{\phi}\\ \ddot{\phi}\end{bmatrix} = \begin{bmatrix} -\frac{I_{eq}C_O}{I_{xx}mV} & -\frac{I_{eq}C_1}{I_{xx}mV^2} - 1 & \frac{h\{mgh-k_r\}}{I_{xx}V} & -\frac{hb_r}{I_{xx}V} \\ -\frac{C_1}{I_{zz}} & -\frac{C_2}{I_{zz}V} & 0 & 0 \\ 0 & 0 & 0 & 1 \\ -\frac{hC_0}{I_{xx}} & -\frac{hC_1}{I_{xx}V} & \frac{mgh-k_r}{I_{xx}} & -\frac{b_r}{I_{xx}} \end{bmatrix}\begin{bmatrix}\beta\\ \dot{\psi}\\ \phi\\ \dot{\phi}\end{bmatrix}$$
$$+ \begin{bmatrix} \frac{I_{eq}C_{af}}{I_{xx}mV} \\ \frac{aC_{af}}{I_{zz}} \\ 0 \\ \frac{hC_{af}}{I_{xx}} \end{bmatrix}\delta + \begin{bmatrix} 0 & 0 & 0 & 0 \\ \frac{d}{2I_{zz}} & -\frac{d}{2I_{zz}} & \frac{d}{2I_{zz}} & -\frac{d}{2I_{zz}} \\ 0 & 0 & 0 & 0 \\ 0 & 0 & 0 & 0 \end{bmatrix}\begin{bmatrix}F_{xrr}\\ F_{xlr}\\ F_{xrf}\\ F_{xlf}\end{bmatrix} \tag{25}$$
$$\triangleq \dot{x}_c \tag{26}$$
$$\triangleq A_c x + B_c u \tag{27}$$
$$y_c \triangleq C_c x \tag{28}$$

This model takes steering angle and longitudinal tire forces as inputs and provides sideslip, yawrate, roll rate and roll angle as outputs. Also, as the height of the center of gravity tends to zero, the model reduces to the planar bicycle model.

For the double lane change maneuvers presented later, the trajectories for this linearization match the nonlinear model trajectories closely. Steering wheel angles remain small at reasonable vehicle speeds and the sideslip angles, lateral forces and longitudinal forces all stay within their linear ranges. For other maneuvers which spend more time at the limits of handling, the linearization will not tend to match the nonlinear model as closely.

For the model predictive control law, the continuous model above discretized with a ZOH will be referred to in the following form.

$$x_k = \begin{bmatrix}\beta_k\\ \dot{\psi}_k\\ \phi_k\\ \dot{\phi}_k\end{bmatrix} \tag{29}$$
$$x_{k+1} = Ax_k + Bu_k \tag{30}$$
$$y_k = Cx_k \tag{31}$$
$$t = k\Delta t, \quad k = 0,\ldots,h \tag{32}$$

where Δt represents the sampling period, x represents the set of vehicle states, k represents the current time epoch.

From the linear equations one can see that the individual braking forces, although consisting of four inputs, only influence the yaw rate $\dot{\psi}$ of the vehicle and even when combined with steering angle, the system is underactuated. This suggests that yaw rate and sideslip may be controlled independently and that all other state trajectories are coupled.

2.4 Assumptions Regarding Sensors and Actuators

The control laws proposed in subsequent sections require several important parameters and measurements to function properly.

The parameters include:

C_x, C_y The tire longitudinal stiffness may be estimated with GPS and stock ABS sensors [8]. GPS and inertial

sensors may be used to estimate the cornering stiffness C_y in real time [5, 7]. Alternately, C_y is sometimes estimated as $\frac{C_x}{2}$ for automobile tires [2].

I_{xx}, I_{zz} The roll and yaw moment of inertia of the vehicle may be estimated using the vehicle mass and its geometry as in [13]. For minivans or SUV's which may have widely varying loads, it may also be necessary to estimate these value in real time.

b_r, k_r The roll stiffness and roll damping may be estimated using automotive grade inertial sensors and GPS [6].

a, b, d, h The center of gravity location, track width wheelbase and roll mode height can be measured by the vehicle manufacturer. For vehicles which largely varying loads such as trucks, it may be necessary to estimate the CG location in real time. Future work will look at explicitly accounting for parameter uncertainty such as this when designing the control law.

The sensors include:

$\beta, \dot{\psi}$ The vehicle sideslip and yaw rate may be measured using a combined GPS and automotive grade inertial system [5–7].

$\phi, \dot{\phi}$ The vehicle roll mode states may also be estimated using a GPS attitude system in combination with an automotive grade gyroscope oriented to measure roll rate [6].

The actuators include:

Steer-by-wire The control law assumes a front wheel steer-by-wire system capable of tracking a desired steering angle command.

Braking The control law assumes that a differential braking system capable of controlling forces at the wheels are available. Although it is not feasible to measure the force produced at the wheels directly for stock automotive systems, it is feasible to estimate the wheel slip. In the linear region, accurate longitudinal stiffness estimates therefore enable force based control of the tires [8].

3 Control Laws

The block diagram for the two control laws presented in this section appears in Figure 3. Both control laws are similar in that they assume the driver's steering angle command corresponds to a desired yaw rate command. They both also solve for the combination of steering and differential braking which will track the driver's desired yaw rate as closely as possible while also preventing the vehicle from exceeding the maximum safe roll angle.

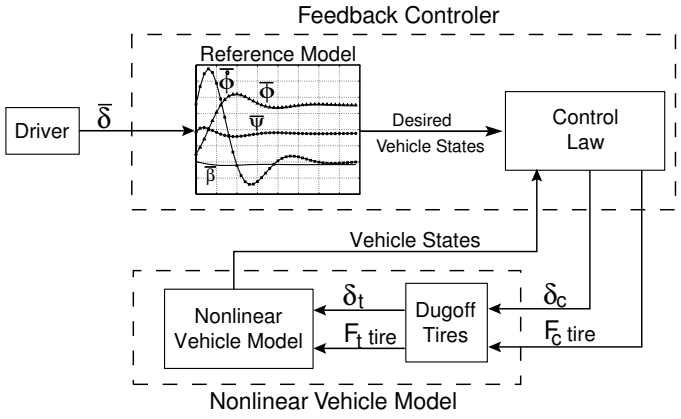

Figure 3. Block diagram of proposed control and simulation structure

The key difference between the two controllers is the information available about the driver's input trajectory. The first, non-causal, control law simply passes the complete input trajectory to the controller structure. In practice it is not possible to know what command a driver will give to the vehicle in the future. However, the response to this input provides an optimal benchmark to which other real time controllers can be compared. The second control law places on a zero order hold on the driver steering command at each time step and calculates the control law for a finite length horizon, similar to the work presented in [2]. This is a more realistic control structure and is implemented with no knowledge of the future steering angle commands.

3.1 Reference Model

Both of the MPC control laws rely on an accurate vehicle model. The model is used to generate a set of desired vehicle state trajectories from the steering angle input command.

When the steering input is known in advance of the maneuver, these trajectories may be completely calculated to the end of the maneuver at each controller time step. In the case where the control input is not completely known, the current steering angle input is held constant and the dynamics are propagated forward over some finite control horizon. Figure 4 shows an example set of state trajectories for a driver input held constant from $t = 0$ to $t = 4$. In practice the horizon length for the unknown input trajectory does not need to be this long; it is typically about 0.15 seconds.

3.2 Tracking Controller Formulation with Constraints

As described earlier, this control law seeks to *closely* track the user's intent while at the same time ensuring that the vehicle roll angle does not exceed the maximum safe value. For this

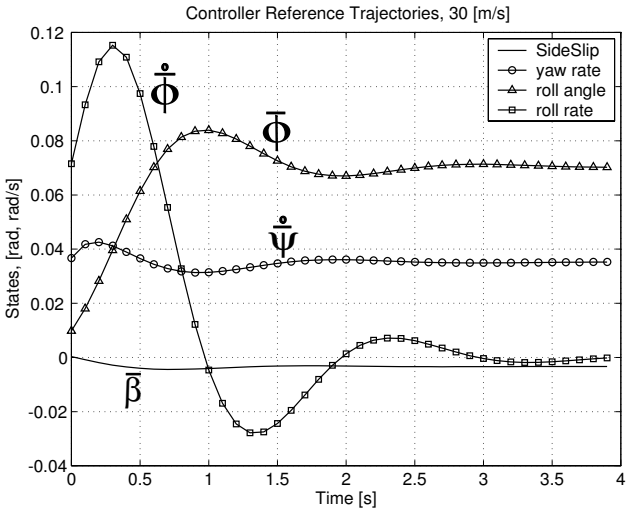

Figure 4. Example of reference trajectories given an input steering angle and some initial condition

work *close* refers to the sum of the squares of the error between the commanded and desired yaw rate trajectory. This idea is nicely expressed in discrete Linear Quadratic Regulator (LQR) language,

$$\underset{U \triangleq \{u_0,\ldots,u_{h-1}\}}{\text{minimize}} \quad J = \sum_{k=0}^{h-1} \left[(y_{k+1} - \bar{y}_{k+1})^T Q (y_{k+1} - \bar{y}_{k+1}) + u_k^T R u_k \right] \tag{33}$$

$$\text{subject to:} \quad x_{k+1} = Ax_k + Bu_k, \quad k = 0,\ldots,h-1 \tag{34}$$

$$y_k = Cx_k, \quad k = 0,\ldots,h \tag{35}$$

$$\bar{y}_k = \bar{C}x_k, \quad k = 0,\ldots,h \tag{36}$$

where y_k is the controlled system tracking output, $\bar{y}_k$ is the reference trajectory to be tracked, and Q, R are the weighting matrices for the square of the tracking error and the square of the input at each discrete time epoch k.

Here the cost function represents the weighted sum of squares of the tracking error, $y_{k+1} - \bar{y}_{k+1}$, with a weighted sum of squares of the input sequence, u_k. The solution to this problem for finite time or infinite time horizons is the input sequence, U. There are many ways to solve this problem and, in particular, there are analytic solutions [14].

What distinguishes the control laws presented here from standard LQR control laws is the ability to explicitly include constraints into the control problem,

$$\text{subject to:} \quad \check{y}_{\min} \le \check{y}_k \le \check{y}_{\max}, \quad k = 1,\ldots,h \tag{37}$$

$$u_{\min} \le u_k \le u_{\max}, \quad k = 0,\ldots,h-1 \tag{38}$$

$$\check{y}_k = \check{C}x_k, \quad k = 0,\ldots,h \tag{39}$$

Where $\check{y}_k$ is the output to be constrained. The inclusion of these constraints explicitly into the control law eliminates many of the design heuristics that accompany LQR control design. In this formulation, constraints on output magnitude, slew rate, input magnitude, input slew rate, etc are all independent of the weighting matrices Q and R. This is also useful for restricting the control law to operating in the linear model and actuator regions.

In general y_k, $\bar{y}_k$ and $\check{y}_k$ may be vectors and may be generated from independent models. However, for this work they are all generated from the same vehicle model. Specifically,

$$y_k \triangleq \dot{\psi}_k \text{ (Controlled output)} \tag{40}$$

$$\bar{y}_k \triangleq \bar{\dot{\psi}}_k \text{ (Desired output)} \tag{41}$$

$$\check{y}_k \triangleq \phi_k \text{ (Hard constrained output)} \tag{42}$$

This choice of trajectories may be interpreted as: control the vehicle output yaw rate, $\dot{\psi}$, to track the reference model yaw rate, $\bar{\dot{\psi}}_k$, closely while maintaining the roll angle output, ϕ_k, within design bounds, $\check{y}_{\max}$ and $\check{y}_{\min}$.

Although this controller configuration tracks yaw rate commands and limits roll angles, this controller structure is much more general. For instance, it could just as easily track desired sideslip, or some weighted combination of sideslip and yaw rate.

Equations 33 - 39 may be re-written in a more directly applicable way. First write the output vectors y_k to the time horizon as a function of the input and the initial state,

$$\begin{bmatrix} y_1 \\ y_2 \\ \vdots \\ y_h \end{bmatrix} = \begin{bmatrix} CB & & \\ CAB & CB & \\ & \vdots & \\ CA^{h-1}B & CA^{h-2}B \cdots & CB \end{bmatrix} \begin{bmatrix} u_0 \\ u_1 \\ \vdots \\ u_{h-1} \end{bmatrix} + \begin{bmatrix} CA^1 \\ CA^2 \\ \vdots \\ CA^h \end{bmatrix} x_0$$

$$\triangleq$$

$$y = SU + Tx_0 \tag{43}$$

The reference trajectory is written in two different forms, depending on whether or not the input is completely known. In the case that it is completely known, it is written,

$$\begin{bmatrix} \bar{y}_1 \\ \bar{y}_2 \\ \vdots \\ \bar{y}_h \end{bmatrix} = \begin{bmatrix} \bar{C}B & & \\ \bar{C}AB & \bar{C}B & \\ & \vdots & \\ \bar{C}A^{h-1}B & \bar{C}A^{h-2}B \cdots & \bar{C}B \end{bmatrix} \begin{bmatrix} r_0 \\ r_1 \\ \vdots \\ r_{h-1} \end{bmatrix} + \begin{bmatrix} \bar{C}A^1 \\ \bar{C}A^2 \\ \vdots \\ \bar{C}A^h \end{bmatrix} x_0$$

$$\triangleq$$

$$\bar{y} = \bar{S}U + \bar{T}x_0 \tag{44}$$

In the case that is not known, it is fixed as constant through a

ZOH and the future dynamics simplify to the following form,

$$\begin{bmatrix} \bar{y}_1 \\ \bar{y}_2 \\ \vdots \\ \bar{y}_h \end{bmatrix} = \begin{bmatrix} \sum_{i=0}^{0} \{\bar{C}\bar{A}^i\bar{B}\} \\ \sum_{i=0}^{1} \{\bar{C}\bar{A}^i\bar{B}\} \\ \vdots \\ \sum_{i=0}^{h-1} \{\bar{C}\bar{A}^i\bar{B}\} \end{bmatrix} \begin{bmatrix} 1 \\ 1 \\ \vdots \\ 1 \end{bmatrix} r + \begin{bmatrix} \bar{C}\bar{A}^1 \\ \bar{C}\bar{A}^2 \\ \vdots \\ \bar{C}\bar{A}^h \end{bmatrix} x_0$$

$$\triangleq$$

$$\bar{y} = \bar{S}r + \bar{T}x_0 \tag{45}$$

The following intermediate variables lead the way to the final compact problem formulation of the reference and vehicle state propagation. Let,

$$Q_d = \text{diag}\,(Q,\ldots,Q) \tag{46}$$

$$R_d = \text{diag}\,(R,\ldots,R) \tag{47}$$

$$H = 2\left(S^T Q_d S + R\right) \tag{48}$$

$$F = \begin{bmatrix} 0 \\ -2\bar{S}^T Q_d S \end{bmatrix} \tag{49}$$

$$Y = \begin{bmatrix} 0 & 0 \\ 0 & -2\bar{S}^T Q_d \bar{S} \end{bmatrix} \tag{50}$$

Lastly, the constraints are written in a compact form as well.

$$G^T = \begin{bmatrix} & I & -I & \\ \bar{S}^T & -\bar{S}^T & \ddots & \\ & & & I \quad -I \end{bmatrix} \tag{51}$$

$$W^T = \begin{bmatrix} \check{y}_{max}^T \ldots \check{y}_{max}^T & -\check{y}_{min}^T \ldots -\check{y}_{min}^T \\ u_{max}^T & -u_{min}^T \ldots u_{max}^T & -u_{min}^T \end{bmatrix} \tag{52}$$

$$E^T = \begin{bmatrix} 0 & 0 & 0 \ldots 0 \\ -\bar{T}^T & \bar{T}^T & 0 \ldots 0 \end{bmatrix} \tag{53}$$

Combining equations 33-45 via the intermediate variables yields the equivalent formulation,

$$\underset{U}{\text{minimize}} \quad J = \frac{1}{2}U^T H U + [x_0^T r^T] F U + \frac{1}{2}[x_0^T r^T] Y \begin{bmatrix} x_0 \\ r \end{bmatrix} \tag{54}$$

$$\text{subject to:} \quad GU \leq W + E \begin{bmatrix} x_0 \\ r \end{bmatrix} \tag{55}$$

This problem formulation is called a Quadratic Program (QP) in U, and when H is positive definite, as it is for the work here, the problem is convex. U for this problem represents the control input vector which will minimize the cost function in Equation 33 while ensuring that the roll angle does not exceed a given preset value. The convexity property of this problem ensures that if a control input exists that satisfies the constraints then it is unique and it can be found efficiently using common computational tools. For a detailed reference on the theory and algorithms which efficiently solve optimization problems of the above form, see [15]. The work here used MATLAB's optimization toolbox for solving these problems.

4 Simulation Results

The vehicle models for these simulations are parameterized to match a minivan's dynamic behavior when travelling at $30[m/s]$. The worst case maximum roll angle is designed not to exceed $0.105[rad]$ during a double lane change maneuver.

4.1 Worst Case Driver Commanded Input

The driver steering command for this example seeks to maximize the peak output of the roll mode in a double lane change maneuver. For a linear system, the following signal, $r(t)$, is known to be the input which will create the largest magnitude output for an input with magnitude bound, $|\delta_{1g}|$:

$$r(t) = |\delta_{1g}|\ sign(g(T-t)) \tag{56}$$

Where $g(t)$ is the impulse response function of the linear system in section 2.3 from steering angle to the roll angle, and T is the given maneuver time of 2.2 seconds. Since the nonlinear model linearizes very well, it is likely this closely matches the worst case input for the nonlinear model as well. To simulate a driver's bandwidth limited response in the worst case, this signal is then low-pass filtered at 3hz . The steering input gain, $|\delta_{1g}|$, is designed to represent a panic lane change maneuver; it is set such that the steady state step response, although not achievable, would yield a $1g$ lateral acceleration.

4.2 Nominal Operation

Figure 5 shows that the control law using the reference input from Equation 44 reproduces the driver's exact commanded trajectory for normal driving conditions. The The top plot shows the commanded and desired yaw rate lie directly on top of one another, the bottom plot shows that the driver commanded steering angle is directly passed through to the steering actuator. The control law which uses Equation 45 performs identically. The following sections show how the vehicle handling behavior is modified for unsafe driver inputs.

4.3 Known Input Trajectory

This controller uses complete knowledge of the driver's input trajectory (Equation 44) so that an optimal benchmark may be set for the best possible controller action. Its response can

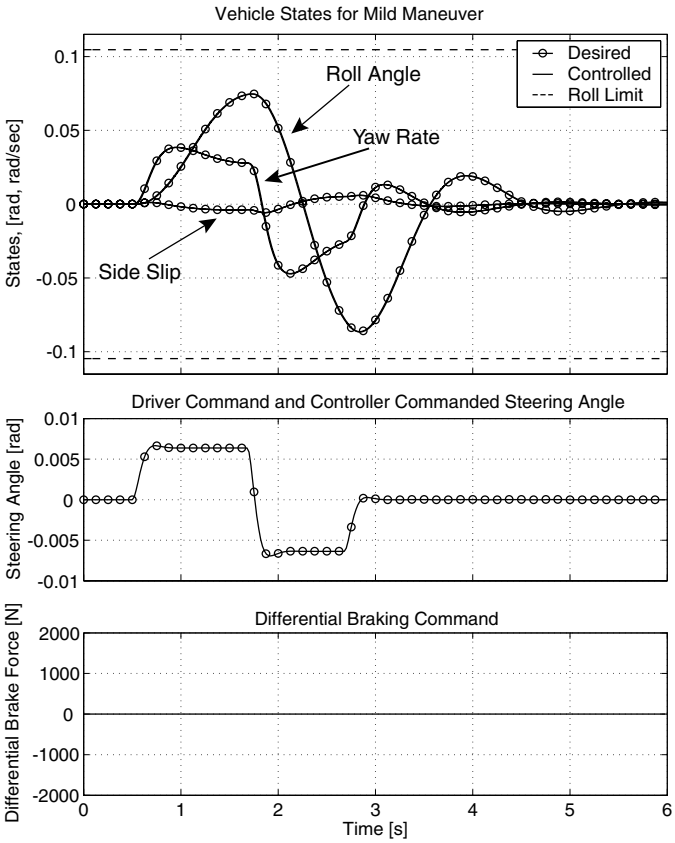

Figure 5. State evolution during normal maneuver

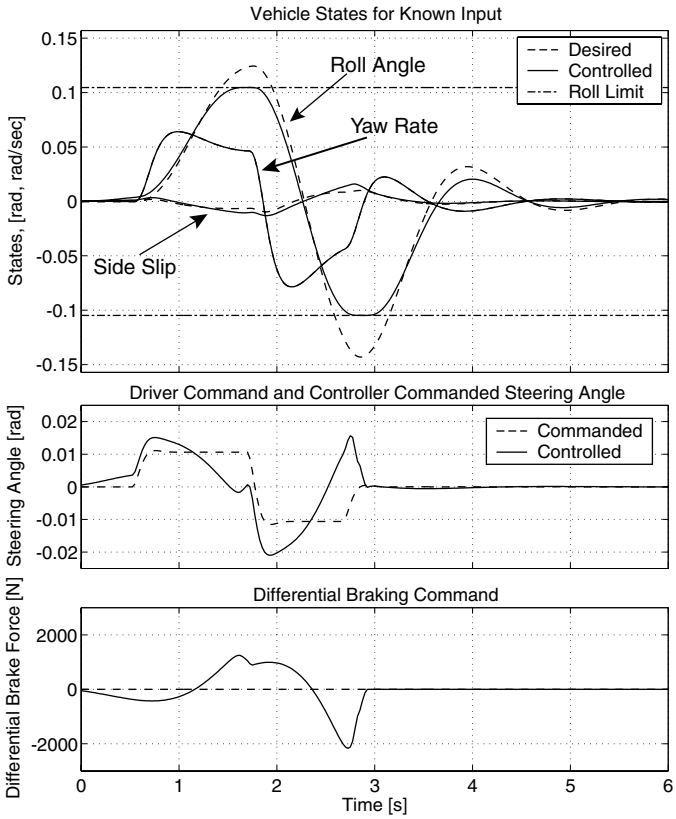

Figure 6. State evolution for known trajectory

be recognized by the differential braking action before the driver begins turning the steering wheel.

Here the control law seeks to limit the roll angle of the vehicle to $0.105[rad]$ while also generating the driver desired yaw rate when the input is completely known in advance. Figure 6 shows the desired and controlled vehicle responses. The figure shows that the control law minimally influences the desired yaw rate trajectory while also limiting the roll angle to less than the desired maximum. In particular the errors between the yaw rate and the desired yaw rate are very small, while the sideslip angle appears to have been minimally affected. It is unlikely the common driver would notice the difference in vehicle response for the maneuver since the trajectory qualitatively maintains it shape, with only a small change in magnitude of the sideslip near the extremes of the maneuver. It is clear that this control law is not causal since the vehicle begins steering an braking well in advance of the driver's steering input.

4.4 Real Time Performance

This second controller has no direct knowledge of the future trajectory (Equation 44.) It knows only the driver's current commanded steering angle and projects the control input forward for a 0.15 second control horizon. Longer time horizons did not change the behavior of the control law significantly and are computationally more expensive. Shorter time horizons, however, resulted in higher peak control effort and larger errors between the commanded and controlled yaw rate.

Once again the control law seeks to limit the roll angle of the vehicle to $0.105[rad]$ while also generating the driver desired yaw rate when only the current commanded input is known. This shows more realistic controller performance since for most applications, the driver's steering command is not known in advance. Figure 7 shows the response of this system and the controller generated inputs. Naturally the control scheme does not deviate from the commanded trajectory until after the driver commands a step steer. It then uses a combination of differential braking and steering to track the yaw-trajectory as much as possible while also limiting the forces into the roll mode. The deviation from the desired trajectory is higher for this case than for the case of a completely known input trajectory, but probably still quite intuitive to the driver. The control law effectively tracks the shape and phase of the driver's commanded yaw rate, but limits the magnitude during portions of the trajectory where the roll angle must be actively limited.

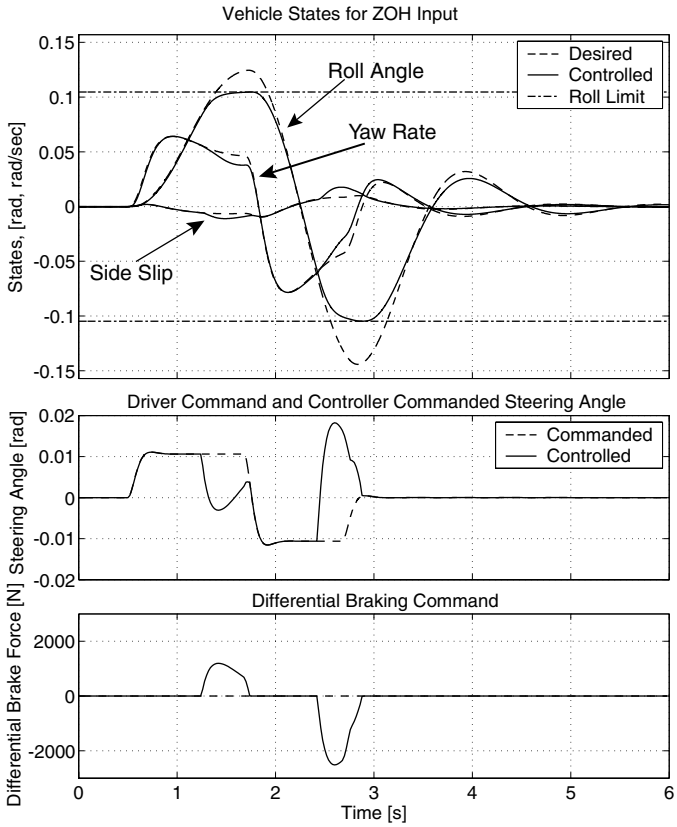

Figure 7. State evolution for ZOH controller

4.5 Explicit Control Law

The control laws as presented in Equation 33 are referred to as *implicit* control laws because they involve solving an optimization problem at every time step. It was recently shown that the solution to this optimal control problem is an *explicit* piecewise affine function of the vehicle state and the control input [10, 11]. Both the implicit and explicit control law formulations are mathematically identical. Thus if computational resources are limited due to processor cost or high sampling rate, *the control law may be explicitly calculated off-line even when the input trajectory is unknown*. This eliminates solving optimization problems in real time which may take longer than the given sample period. Once computed, the control law implementation consists of a series of if-then statements, with each statement representing an affine control law for a convex portion of the state space.

For this application, the explicit control law breaks up the state space into approximately 500 convex regions, each associated with a different affine control law. Evaluating the control law simply consists of checking which of the 500 regions the vehicle states currently lie in and then evaluating the feedback law associated with that region. However, for this maneuver 99% of time, the control flipped between two distinct operating regions. Looking at these two regions in detail gives valuable intuition about how the control law functions. During the time history of the vehicle states in Figure 7, they passed primarily through the following regions.

$$0 \le t \le 1.24 \quad \text{Region 1} \tag{57}$$
$$1.24 < t \le 1.72 \quad \text{Region 2} \tag{58}$$
$$1.72 < t \le 2.44 \quad \text{Region 1} \tag{59}$$
$$2.44 < t \le 2.88 \quad \text{Region 2} \tag{60}$$
$$2.88 < t \le 6 \quad \text{Region 1} \tag{61}$$

For the first region, the feedback law is,

$$^1u_k = \begin{bmatrix} 0 \\ 0 \end{bmatrix} + \begin{bmatrix} 0 & 0 & 0 & 0 & 1 \\ 0 & 0 & 0 & 0 & 0 \end{bmatrix} \begin{bmatrix} x_k \\ r \end{bmatrix} \tag{62}$$

where row one of the control input at time epoch k is the command to the steer-by-wire system, and row two is the command to the differential braking system in kilonewtons. It is clear that inside region 1 the control law would be completely transparent to the driver. The control law simply feeds the driver's steering angle measurement directly into the steer-by-wire system.

Region 2 represents the case where the roll angle would nominally exceed the design bounds,

$$^2u_k = \begin{bmatrix} 0.194 \\ -16.961 \end{bmatrix} + \begin{bmatrix} 2.25 & -0.14 & -1.53 & -0.20 & -0.49 \\ -196.0 & 12.4 & 133.2 & 17.6 & 130.1 \end{bmatrix} \begin{bmatrix} x_k \\ r \end{bmatrix} \tag{63}$$

In this region the control law actively applies both steering and differential braking commands to the vehicle.

The control action of this controller may be intuitively understood with a thought experiment. First assume that the steering command reference makes a step change from zero to some positive steady state value. As the dynamics develop, the roll angle and yaw rate are positive while the sideslip is negative. Then, if the forward propagation of the dynamic reference model will result in too high of a roll angle, the controller switches to Region 2 gains. The first row of the Region 2 gains, which correspond to the steering input, have the opposite sign of the vehicle states. This implies that the controller understeers the reference command. The differential braking command, however, has the same signs as the vehicle states. This implies that the differential braking is making up for lost yaw rate due to understeer by directly yawing the vehicle. The combined result of this control action is also intuitive. The desired yaw rate is effectively tracked while the vehicle sideslip, is reduced from the driver commanded value. This effectively reduces the energy introduced to the base of the roll mode and therefore limits the peak roll angle.

5 Conclusions

There is a significant opportunity to improve the safety of the current vehicle fleet by preventing vehicle rollover. New GPS based sensing technology and actuator technology enables the use of nonlinear optimal control methods. Although the simulation studies are far from exhaustive, the early results showing the performance of these methods are encouraging. They show that if the input trajectory is completely known, it is possible via steer-by-wire and differential braking to track the drivers intent extremely closely while maintaining a safe roll angle. They also show it is possible to closely track the driver's intent in real time without knowledge of the future steering commands while also maintaining a safe roll angle. Explicitly solving for the control law for the real time case also reveals the control action appears quite simple for this maneuver.

6 Future Work

The simulation results demonstrated here were far from exhaustive, and neglect many real world effects, such as suspension kinematics and camber change, during the presented dynamic vehicle maneuvers. Additionally, they are difficult to really kinesthetically understand from a driver's perspective. Future work will implement these controller structures on a test vehicle with fully by-wire steering and independent electric drive motors in each of the rear wheels.

Although the GPS based sensing and estimation schemes proposed for this work do provide accurate parameter estimates and state measurements, they are still uncertain. Future work will seek to analytically guarantee vehicle safety in the presence of bounded parameter and measurement uncertainty.

The proposed control law, while optimal in some sense is still very complicated and sometimes difficult to intuitively understand. However, during certain regions of operation, its control actions are intuitively quite transparent. Future work will look at finding possibly suboptimal control laws with more direct design intuition.

Finally, although the control laws here choose to follow a model which closely matches the controlled vehicle's dynamics. It is perfectly feasible to place another dynamic model in its place. Future work will look at changing the dynamic behavior of by-wire vehicles via MPC.

7 Acknowledgements

The authors would like to thank the reviewers for their thoughtful comments on the first draft of this paper. We also acknowledge DaimlerChrysler for supporting of this research.

REFERENCES

[1] Jeffery W. Runge. Before the Committee On Commerce Science and Transportation: United States Senate . *Available from http://www.nhtsa.dot.gov/hot/FinalSUVStatement.html*.

[2] A. T. van Zanten. Evolution of Electronic Control Systems for Improving the Vehicle Dynamic Behavior. In *Proceedings of the* 6^{th} *International Symposium on Advanced Vehicle Control*, 2002.

[3] Bo-Chiuan Chen and Huei Peng. Differential-Braking-Based Rollover Prevention for Sport Utility Vehicles with Human-in-the-loop Evaluations. In *Vehicle System Dynamics*, volume 36, 4-5, pages 359–389, 2001.

[4] Thomas J. Wielenga and Milton A. Chace. A Study in Rollover Prevention Using Anti-Rollover Braking. In *SAE Technical Paper Series 2000-01-1642*, 2000.

[5] D. M. Bevly, R. Sheridan, and J. C. Gerdes. The Use of GPS Based Velocity Measurements for Improved Vehicle State Estimation. In *Proceedings of the American Control Conference, Chicago IL*, pages 2538–2542, 2000.

[6] Jihan Ryu, Eric J. Rossetter, and J. Christian Gerdes. Vehicle Sideslip and Roll Parameter Estimation Using GPS. In *Proceedings of AVEC 2002* 6^{th} *International Symposium of Advanced Vehicle Control*, 2002.

[7] Jin-Oh Hahn and Rajesh Rajamani. GPS-Based Real-Time Identification of TireRoad Friction Coefficient. *IEEE Transactions on Control System Technology*, 10, NO.3:331–343, MAY 2002.

[8] Christopher R. Carlson and J. Christian Gerdes. Nonlinear Estimation of Longitudinal Tire Slip Under Several Driving Conditions. In *Proceedings of the 2003 American Control Conference, Denver, CO*, pages 4975–4980, 2003.

[9] S. J. Qin and Badgwell. An overview of industrial model predictive control technology. In *Chemical Process Control*, volume 93, 316, pages 232–356, 1997.

[10] A. Bemporad, M. Morari, V. Dua, and E. N. Pistikopoulos. The Explicit Linear Quadratic Regulator for Constrained Systems. *Automatica*, 38(1):3–20, 2002.

[11] P. Grieder, F. Borrelli, F. Torrisi, and M. Morari. Computation of the Constrained Infnite Time Linear Quadratic Regulator. In *Proceedings of the 2003 American Control Conference, Denver, CO*, pages 4711–4716, 2003.

[12] Howard Dugoff, P.S. Francher, and Leonard Segel. An Analysis of Tire Traction Properties and Their Influence on Vehicle Dynamic Performance. *SAE Document Number Document 700377*, 1970.

[13] Michael W. Monk W. Riley Garrott and Jeffrey P. Chrstos. Vehicle Inertial Parameters Measured Values and Approximations. *SAE Paper No. 881767*.

[14] Robert F. Stengel. *Optimal Control and Estimation*. Dover Publications, New York, 1986.

[15] Stephen Boyd and Lieven Vandenberghe. *Convex Optimization*. http://www.stanford.edu/ boyd/cvxbook.html, 2003.